

Influence of stimulated processes on the properties of the Hanle signal. Investigation of spectra

F. A. Lomaya and A. A. Pantelev

Troitsk Institute of Innovative and Thermonuclear Research, 142092 Troitsk, Moscow Region, Russia
(Submitted 20 April 1994)

Zh. Eksp. Teor. Fiz. **106**, 886–903 (September 1994)

The influence of stimulated absorption and emission processes, as well as four-wave mixing, on the fluorescence spectra of atoms excited by a monochromatic wave of arbitrary intensity in a magnetic field has been studied. Investigations have been performed for scattering of the incident wave on an optically dense atomic beam and on an optically thin beam when the fluorescence photons assemble in a high- Q cavity. The spectral dependence of the absorption and four-wave mixing coefficients, which determine the dynamics of the stimulated processes, has been examined. The special features of the probe-wave method as applied to the system under consideration have been discussed. The importance of the four-wave mixing processes accompanying the interference phenomena has been noted. The special features of the phase matching corresponding to these processes have been investigated. The results obtained have been used to describe the modification of spectra of the Hanle signal due to the influence of stimulated processes.

1. INTRODUCTION

Expressions describing the spectral characteristics of the Hanle effect^{2,3} for a monochromatic wave of arbitrary intensity in a $J=0 \rightarrow J=1$ transition were recently obtained in Ref. 1. Resonance fluorescence spectra for a monochromatic wave of arbitrary intensity were first obtained by Rautian and Sobel'man⁴ for scattering on an open two-level system and by Mollow for a two-level atom.⁵ It was shown that the emission spectra of an atom undergo significant changes in a strong wave field and have the form of a triplet of Lorentzians detuned from the generalized Rabi frequency. It should be noted that the absorption spectra also change significantly, and in some regions absorption may be replaced by amplification.⁶ It was shown in Ref. 1 that the spectrum of the Hanle signal for an intense monochromatic wave in a $J=0 \rightarrow J=1$ transition may contain up to seven resonances, which are a consequence of the splitting of the three-level system in the strong field (see Fig. 1a).

The investigations of the properties of the Hanle effect performed in Ref. 1, as well as in Refs. 3 and 7–9 and in most of the other studies, suggest that atoms spontaneously scatter the incident radiation in free space. The dimensions of the medium or, more precisely, its optical thickness, are assumed to be small. This means that stimulated emission processes may be neglected in describing the scattered radiation. The present work was devoted to an investigation of the influence of stimulated processes on spectra of the Hanle signal.

Fabry–Perot cavities are often used in laser spectroscopy to precisely measure the frequency. In high- Q cavities, stimulated processes become significant due to the presence of feedback even in initially optically thin media, such as, for example, atomic beams. These processes include absorption (amplification) of the scattered radiation and multiwave mixing. We note that the influence of a cavity on the resonance fluorescence spectra of a two-level atom was investigated in

Ref. 10. It is also clear that stimulated processes are very important for scattering in optically dense media.

Figure 1b presents a possible scheme for an experimental investigation of the spectral properties of the Hanle effect. We assume that an intense monochromatic wave is linearly polarized along the y axis and propagates along the x axis. A constant magnetic field is directed along the z axis. The Hanle signal; i.e., x -polarized resonance fluorescence, is observed in the y direction, and we assume that the atomic beam (A1) propagates along the z axis (See Fig. 1b). We shall also analyze the spectra of the y -polarized fluorescence along the z axis. In this case we assume that the atomic beam (A2) propagates along the x axis. This experimental measurement scheme makes it possible to avoid the influence of the Doppler effect on the scattering spectra. We investigated the role of stimulated processes as applied to intracavity spectroscopic methods under the assumption that the scattering system is in the cavity (it is not shown in the figure), which is oriented in the line of sight. In addition, in the present work we investigated scattering spectra in an optically dense atomic beam. Here it is assumed that the cross-sectional dimensions of the latter are much smaller than the diameter of the laser beam. This permits neglect of the non-uniformity of the laser field in the cross section of the atomic beam.

We use the formalism developed Refs. 1 and 11, where a method which is based on the quantum theory of multiwave mixing^{12,13} and makes it possible to investigate the polarization effects of a resonant interaction of several waves was described. This theory makes it possible to describe the polarization properties of a nonlinear interaction between waves, probe-field spectroscopy, resonance fluorescence, and other phenomena in quantum and nonlinear optics.

The principal equations for describing the Hanle effect, which were derived in Refs. 1 and 11, will be presented in Sec. 2. The absorption and four-wave mixing coefficients of the spectrally degenerate modes which determine the dynam-

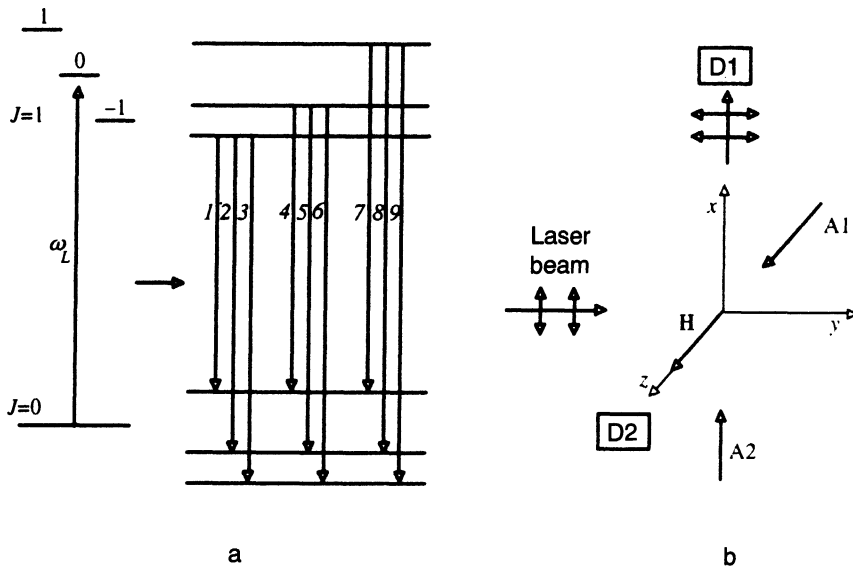


FIG. 1. a) Displacement and splitting of the atomic energy levels of a $J=0 \rightarrow J=1$ system under the action of a strong monochromatic wave in a constant magnetic field. The lines corresponding to transitions 3, 5, and 7 are spectroscopically degenerate with the frequency of the exciting radiation. b) Possible experimental setup for observing the Hanle effect. The vector \mathbf{H} defines the direction of the magnetic field, $A1$ and $A2$ are atomic beams, and $D1$ and $D2$ are detectors of the scattered radiation.

ics of the stimulated processes in the problem under consideration here will be considered in Sec. 3. The influence of the cavity on the fluorescence spectra will be investigated in Sec. 4. In Sec. 5 the role of propagation effects on the fluorescence spectra observed when a laser wave is scattered in an optically dense atomic beam will be examined. The role of four-wave mixing and the features of the wave-vector matching will also be investigated. The main conclusions and results of the work will be presented in Conclusions.

2. PRINCIPAL EQUATIONS

In the rotating-wave and dipole-interaction approximations, the Hamiltonian of the system under consideration has the form (in rad/s)

$$H = \Delta_L R_e + \sum_{j,\sigma} \nu_j a_{j\sigma}^+ a_{j\sigma} + \Omega R_z + \sum_{\sigma} (V_{\sigma} R_{\sigma 0}^+ + V_{\sigma}^* R_{0\sigma}^-) + \sum_{j,\sigma} (g_{j\sigma} R_{\sigma 0}^+ U_{j\sigma} a_{j\sigma} + g_{j\sigma}^* R_{0\sigma}^- U_{j\sigma}^* a_{j\sigma}^+), \quad (1)$$

where $a_{j\sigma}$ is the annihilation operator for photons in the j th mode having a wave vector $\mathbf{k}_{j\sigma}$ with left-handed ($\sigma=+$) and right-handed ($\sigma=-$) polarization and a frequency ω_j . In these expressions $\Delta_L = \omega_0 - \omega_L$, $\nu_j = \omega_j - \omega_L$, ω_0 is the transition frequency, and ω_L is the frequency of the laser wave, which is linearly polarized along the y axis (see Fig. 1). The first two terms in expression (1) define the Hamiltonians of the unperturbed atomic subsystem and the quantum radiation field. The third term describes the effect of the magnetic field on the atoms, Ω being the Larmor frequency. The fourth term in expression (1) describes the interaction of the atoms with the laser wave, which we have represented in the form of a sum of σ components with electric field strengths E_{σ} . Here

$$V_{\sigma} = -\mu_{\sigma 0} E_{\sigma} U_L / 2\hbar,$$

where $\mu_{\sigma 0}$ is the matrix element of the dipole moment in the $|0\rangle \rightarrow |\sigma\rangle$ transition. The vector $|0\rangle$ describes the lower state of the atom, and $|\sigma\rangle$ describes the upper state $|+\rangle$ with $m_j = +1$

or $|-\rangle$ with $m_j = -1$. In the calculations we assume that $|V_+| = |V_-| = V$. The last term in Hamiltonian (1) describes the interaction of the atoms with the quantum electromagnetic field. The function $U_j = U_j(\mathbf{r})$ describes the spatial distribution of the j th mode;

$$g_{j\sigma} = -i\mu_{\sigma 0} \sqrt{2\pi\omega_j / c\hbar W}$$

is the coupling constant, where W is the quantization volume. The atomic system is described using the matrices R from Ref. 1, which are three-dimensional generalizations of the 2×2 Pauli matrices for use in the three-level system shown in Fig. 1a. They satisfy the commutation relations

$$[R_e, R_{\sigma 0}^+] = 2R_{\sigma 0}^+, \quad [R_e, R_{0\sigma}^-] = -2R_{0\sigma}^-, \\ [R_z, R_{\sigma 0}^+] = \sigma R_{\sigma 0}^+, \quad [R_z, R_{0\sigma}^-] = -\sigma R_{0\sigma}^-, \quad (2)$$

and their effect on the eigenfunctions of the atomic subsystem is specified by the expressions

$$R_{\sigma 0}^+ |\sigma'\rangle = |\sigma\rangle \delta_{\sigma'\sigma}, \quad R_{0\sigma}^- |\sigma'\rangle = |0\rangle \delta_{\sigma'\sigma}, \quad (3)$$

where $\delta_{\sigma\sigma'}$ is the Kronecker delta.

The components of the atomic density matrix ρ are defined in the following manner:

$$\rho_{0\sigma} = \langle R_{\sigma 0}^+ \rho \rangle, \quad \rho_{\sigma'\sigma} = \langle R_{\sigma 0}^+ R_{0\sigma'}^- \rho \rangle, \\ \rho_{\sigma 0} = \langle R_{0\sigma}^- \rho \rangle, \quad \rho_{00} = \langle R_{0\sigma}^- R_{\sigma 0}^+ \rho \rangle \delta_{\sigma\sigma'}. \quad (4)$$

We note that expressions (4) differ from the analogous expressions in Refs. 1 and 11. This is due to the different definitions of the eigenfunctions of the atomic subsystem: in Refs. 1 and 11 the kets $|\sigma\rangle$ were defined as row vectors, and in the present work we define them, as has generally been done in the literature, as column vectors [see (3)]. These differences do not alter the physical results.

Let us define the atom-photon operator ρ_{a-ph} of an atom + field system. For this purpose we take the standard equation of motion¹²⁻¹⁴

$$i\dot{\rho}_{a-ph}=[H,\rho_{a-ph}]+i\Gamma(\rho_{a-ph}), \quad (5)$$

where the operator $\Gamma(\rho_{a-ph})$ describes the relaxation processes. We have the following equation of motion for the atomic density matrix ρ without consideration of the interaction with the quantum modes:

$$i\dot{\rho}=\mathbf{M}\rho, \quad (6)$$

where $\rho^\dagger=(\rho_{++},\rho_{--},\rho_{00},\rho_{0+},\rho_{+0},\rho_{0-},\rho_{-0},\rho_{+-},\rho_{-+})$, and the matrix \mathbf{M} has the form

$$\mathbf{M}=\begin{pmatrix} -i\gamma & 0 & 0 & V_+ & -V_+^* & 0 & 0 & 0 & 0 \\ 0 & -i\gamma & 0 & 0 & 0 & V_- & -V_-^* & 0 & 0 \\ i\gamma & i\gamma & 0 & -V_+ & V_+^* & -V_- & V_-^* & 0 & 0 \\ V_+^* & 0 & -V_+^* & \Delta_+^* & 0 & 0 & 0 & 0 & V_-^* \\ -V_+ & 0 & V_+ & 0 & -\Delta_+ & 0 & 0 & -V_- & 0 \\ 0 & V_-^* & -V_-^* & 0 & 0 & \Delta_-^* & 0 & V_+^* & 0 \\ 0 & -V_- & V_- & 0 & 0 & 0 & -\Delta_- & 0 & -V_+ \\ 0 & 0 & 0 & 0 & -V_-^* & V_+ & 0 & \delta^* & 0 \\ 0 & 0 & 0 & V_- & 0 & 0 & -V_+^* & 0 & -\delta \end{pmatrix}, \quad (7)$$

where $\Delta_\pm=\omega_L-\omega_0\mp\Omega+i\gamma/2$, $\delta=2\Omega+i\gamma$, and γ is the rate of spontaneous relaxation. Since the atomic subsystem is closed, system (6), which is linearly dependent, must be supplemented with the condition $\text{Tr } \rho=1$.

The operator of the photon field P is determined from the operator ρ_{a-ph} by taking the trace with respect to the atomic states. The equation of motion for the slowly varying component of this operator in second-order perturbation theory with respect to the coupling constant g has the form¹¹⁻¹³

$$\begin{aligned} \dot{P} &= \sum_{j,\sigma,\sigma'} [A_{j\sigma,j\sigma'}(a_{j\sigma}^+ P a_{j\sigma'} - P a_{j\sigma'} a_{j\sigma}^+) \\ &+ (B_{j\sigma,j\sigma'} + \delta_{\sigma\sigma'} \omega_j / 2Q_j)(a_{j\sigma'} P a_{j\sigma}^+ - a_{j\sigma}^+ a_{j\sigma'} P)]. \end{aligned} \quad (8)$$

Here, the rate of intracavity loss is taken into account for the case in which the system is in the cavity. The quantity Q_j describes the Q factor of the cavity for the j th mode. The coefficients A and B are determined below [see (14)–(17)].

In this equation we omitted the group of terms which describe the four-wave mixing processes in the direction of propagation of the incident wave (see Ref. 11). This is due to the fact that the geometry of the Hanle effect considered in this work is such (see Fig. 1b) that the conditions for the realization of wave-vector matching in the four-wave mixing processes involving the incident wave and the scattered waves symmetrically detuned from it do not exist.^{12,13}

In the problem under consideration, along with the mean

$$\langle a_{j\sigma}^+ a_{j\sigma} \rangle = \langle a_{j\sigma}^+ a_{j\sigma} P \rangle = n_{j\sigma}$$

($n_{j\sigma}$ is the number of the photons with the wave vector $\mathbf{k}_{j\sigma}$), the correlators $\langle a_{j\sigma}^+, a_{j\sigma'} \rangle$ ($\sigma \neq \sigma'$) are also significant. The existence of these correlators, which is associated with the coherence introduced into this system by the pump wave,

makes it possible to describe the interference effects that are significant, in particular, in the Hanle effect. The appearance of these correlators requires fulfillment of the following condition:

$$(\mathbf{k}_{j+} - \mathbf{k}_{j-} + \mathbf{k}_{L-} - \mathbf{k}_{L+}) \mathbf{r} = 0. \quad (9)$$

Since $\mathbf{k}_{j+} \approx \mathbf{k}_{j-}$ and $\mathbf{k}_{L-} \approx \mathbf{k}_{L+}$, condition (9) can essentially always be considered satisfied.

The equations of motion for the photon numbers and the quantum correlators of photons with different polarization have the form

$$\frac{d}{dt} n_+ = \alpha'_+ n_+ + \beta_+ \langle a_+^+ a_- \rangle + A_{++} + \text{h.c.}, \quad (10)$$

$$\frac{d}{dt} n_- = \alpha'_- n_- + \beta_- \langle a_-^+ a_+ \rangle + A_{--} + \text{h.c.}, \quad (11)$$

$$\begin{aligned} \frac{d}{dt} \langle a_-^+ a_+ \rangle &= (\alpha'_-{}^* + \alpha'_+) \langle a_-^+ a_+ \rangle + \beta_-^* n_+ + \beta_+ n_- \\ &+ A_{-+} + A_{+-}^*, \end{aligned} \quad (12)$$

$$\begin{aligned} \frac{d}{dt} \langle a_+^+ a_- \rangle &= (\alpha'_+{}^* + \alpha'_-) \langle a_+^+ a_- \rangle + \beta_+^* n_- + \beta_- n_+ \\ &+ A_{+-} + A_{-+}^*, \end{aligned} \quad (13)$$

where $\alpha'_\sigma = a_\sigma - \omega/2Q$, $\alpha_\sigma = A_{\sigma\sigma} - B_{\sigma\sigma}$, $\beta_\sigma = A_{\sigma\sigma'} - B_{\sigma\sigma'}$, and it is assumed that $\sigma \neq \sigma'$. For the scattering of radiation in free space, α' is replaced by α . The index j is omitted here and below, since spectrally degenerate modes are coupled.

The coefficients A and B are defined in the following manner:

$$A_{++} = iN |g_+|^2 (z_{35} \rho_{0+} + z_{55} \rho_{++} + z_{75} \rho_{-+}), \quad (14)$$

$$B_{++} = iN |g_+|^2 (-z_{15} \rho_{0+} - z_{55} \rho_{00} + z_{85} \rho_{0-}), \quad (15)$$

$$A_{+-} = iNg - g_+^*(z_{35}\rho_{0-} + z_{55}\rho_{+-} + z_{75}\rho_{--}), \quad (16)$$

$$B_{+-} = -iNg - g_+^*(z_{25}\rho_{0-} - z_{75}\rho_{00} - z_{95}\rho_{0+}), \quad (17)$$

where ρ_{jk} is the stationary solution of system (6), $z_{jk} = \det Z_{jk} / \det Z$, and Z_{jk} is the minor of the matrix $Z = M + \nu I$ (here I is the unit matrix), $\nu = \omega - \omega_L$, and N is the number of atoms. The corresponding coefficients for $\sigma = -$ are obtained by making the replacements $\Omega \rightarrow -\Omega$, $V_+ \leftrightarrow V_-$.

Equations (10)–(13) make it possible to describe the Hanle effect, i.e., the fluorescence in the system shown in Fig. 1b. The photons with left- and right-handed polarization are specified by the photon numbers n_+ and n_- , and their fluorescence spectra are specified by \mathcal{A}_{++} and \mathcal{A}_{--} . Here $\mathcal{A}_{\sigma\sigma'} = A_{\sigma\sigma'} + A_{\sigma'\sigma}^*$. The Hanle signal is determined by the number of photons with linear polarization in the x direction, and the fluorescence spectrum is, accordingly, determined by \mathcal{A}_x . Using the relationship between the creation operators of photons with circular polarization and photons with linear polarization, we have the following relations for the photon numbers:

$$n_x = n_+ + n_- - \langle a_+^\dagger a_- \rangle - \langle a_-^\dagger a_+ \rangle, \quad (18)$$

$$n_y = n_+ + n_- + \langle a_+^\dagger a_- \rangle + \langle a_-^\dagger a_+ \rangle. \quad (19)$$

Photons with x polarization are observed in the y direction, and photons with y polarization are observed in the z direction (see Fig. 1). The overall expression for the number of photons with linear polarization in the ye plane (the vector e specifies the direction of photon scattering) has the form

$$\begin{aligned} n = (n_+ + n_-)(1 - \cos^2 \theta \sin^2 \varphi) + (\sin^2 \theta \\ - \cos^2 \varphi \cos^2 \theta)(\langle a_+^\dagger a_- \rangle + \langle a_-^\dagger a_+ \rangle) \\ + i \sin 2\theta \cos \varphi (\langle a_+^\dagger a_- \rangle - \langle a_-^\dagger a_+ \rangle). \end{aligned} \quad (20)$$

Here θ is the angle which the vector e forms with the y axis, and φ is the angle between its projection onto the xz plane and the x axis.

For an optically thin system, in which the stimulated processes can be neglected, we have

$$n_x \propto \mathcal{A}_x = \mathcal{A}_{++} + \mathcal{A}_{--} - \mathcal{A}_{+-} - \mathcal{A}_{-+}, \quad (21)$$

$$n_y \propto \mathcal{A}_y = \mathcal{A}_{++} + \mathcal{A}_{--} + \mathcal{A}_{+-} + \mathcal{A}_{-+}. \quad (22)$$

These spectra were thoroughly scrutinized in Ref. 1.

The total intensity of the Hanle signal is given by

$$J_x \propto \int \mathcal{A}_x d\nu \alpha \rho_{++} + \rho_{--} - \rho_{+-} - \rho_{-+}, \quad (23)$$

and, accordingly,

$$J_y \propto \int \mathcal{A}_y d\nu \alpha \rho_{++} + \rho_{--} + \rho_{+-} + \rho_{-+}. \quad (24)$$

These quantities were investigated by Avan and Cohen-Tannoudji.⁷

It is noteworthy that since the lower level corresponds to the ground state in the atomic subsystem considered here, two components can be identified in the fluorescence spectra: an elastic or undisplaced component, which is proportional

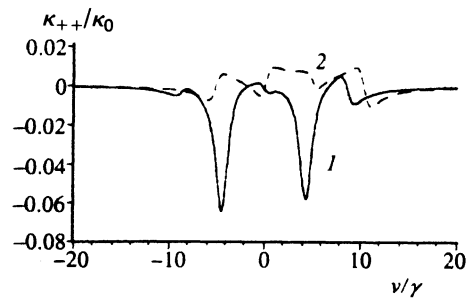


FIG. 2. Spectral dependence of κ_{++} for $V/\gamma=3$, $\Delta_L=0$, and $\Omega/\gamma=1$ (curve 1) and 3 (curve 2).

to $\delta(\nu)$, and an inelastic component, which describes scattering with a change in photon frequency. We write the expressions for the fluorescence spectra in the form

$$\mathcal{A}_{\sigma\sigma'} = \mathcal{A}_{\sigma\sigma'}^{el} + \mathcal{A}_{\sigma\sigma'}^{inel}, \quad (25)$$

$$\mathcal{A}_x = \mathcal{A}_x^{el} + \mathcal{A}_x^{inel}. \quad (26)$$

The elastic component $\mathcal{A}_{\sigma\sigma'}^{el}$ is

$$\mathcal{A}_{\sigma\sigma'}^{el} = 2\pi N g_{\sigma'}^* g_{\sigma} \rho_{0\sigma} \rho_{\sigma'0} \delta(\nu). \quad (27)$$

For the elastic component of the Hanle signal \mathcal{A}_x^{el} , we therefore have

$$\mathcal{A}_x^{el} = 2\pi N |g_+ \rho_{0+} - g_- \rho_{0-}|^2 \delta(\nu). \quad (28)$$

In the weak-field limit $V \ll \gamma$ this component is decisive, and in this case expression (28) corresponds to the well known result for the Hanle signal,^{3,15} which follows from second-order perturbation theory.

It should be noted that a nonstandard representation of the polarization structure of an electromagnetic field was used in the foregoing description based on the results in Refs. 1 and 11, since in the present work, as in Refs. 1 and 11, the incident wave was represented in the form of a sum of σ components, while in the standard description³ it is proportional to their difference. A nonstandard representation was also used for the creation and annihilation operators of the photons with σ polarization. We can show how the equations derived here are modified when the standard description of the polarization structure of an electromagnetic wave is used. Under the conditions of the geometry considered here, the traditional expressions for the photon operators have the form

$$a_{\pm} = \mp \frac{1}{\sqrt{2}} (a_y \pm i a_x).$$

Taking this definition into account, in Eqs. (18)–(24) and (28) we should reverse the overall sign in front of the terms containing interference terms, i.e., with $\sigma \neq \sigma'$, and multiply the entire right-hand side by $1/2$. We note that the physically measured quantities (e.g., the intensity and spectrum of the scattered radiation), of course, do not depend on the representation.

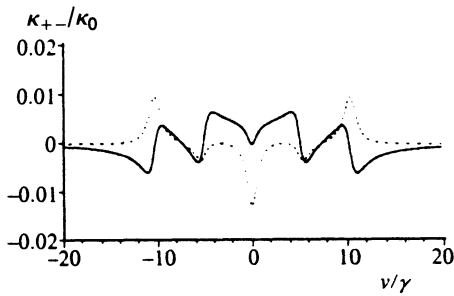


FIG. 3. Spectral dependence of the real (solid line) and imaginary (dashed line) parts of κ_{+-} for $V/\gamma=3$, $\Delta_L=0$, and $\Omega/\gamma=3$.

3. INVESTIGATION OF STIMULATED PROCESSES

The coefficients α_σ and β_σ in Eqs. (10)–(13) describe stimulated processes: absorption (amplification) of radiation and four-wave mixing. Figures 2–4 present plots of the spectral dependence of the absorption coefficients κ_{++} and κ_{+-} ($\kappa_{\sigma\sigma'} = \alpha_\sigma + \alpha_{\sigma'}^*$), as well as β_+ , for various values of V/γ and Ω/γ and exact resonance of the pump wave with the transition frequency $\Delta_L=0$. These quantities are generally not understood to be the absorption and four-wave mixing coefficients, and in Eqs. (10)–(13) they describe the rates of these processes. The corresponding absorption and four-wave mixing coefficients are obtained by dividing by the phase velocity of light. All the spectra in Figs. 2–4 were normalized to the unperturbed ($E_L=0$, $\Omega=0$) absorption rate κ_0 at the line center ($\omega=\omega_0$). These figures reveal that in intense fields, the spectra of these coefficients have a complicated structure and many features. This is attributed to the splitting of the atomic subsystem in the strong electromagnetic field (see Fig. 1a),^{1,11} and the features in the spectra of the coefficients are located near components corresponding to the generalized Rabi frequencies. We note that α_σ and β_σ satisfy the Kramers–Kronig relations,¹⁶ while κ_{+-} does not (see Fig. 3).

We note that the $\kappa_{\sigma\sigma'}$ cannot be interpreted strictly as absorption coefficients. This is due to the fact that the appearance of photons with a wave vector \mathbf{k}_σ in the medium induces polarization for photons with a wave vector $\mathbf{k}_{L\sigma'} - \mathbf{k}_{L\sigma} + \mathbf{k}_\sigma \approx \mathbf{k}_{\sigma'} (\sigma \neq \sigma')$.

Let us investigate this phenomenon in greater detail for the example of classical probe fields.¹⁷ Following Ref. 12,

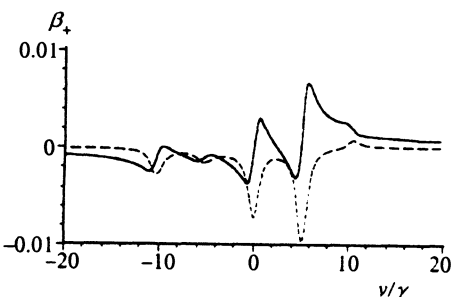


FIG. 4. Spectral dependence of the real (solid line) and imaginary (dashed line) parts of β_+ for $V/\gamma=3$, $\Delta_L=0$, and $\Omega/\gamma=3$.

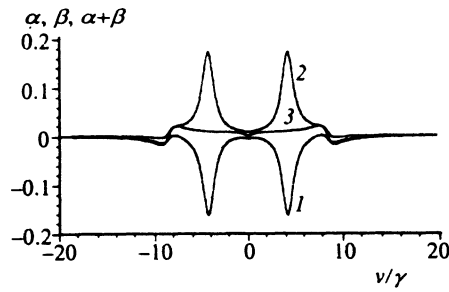


FIG. 5. Spectral dependence of α (curve 1), β (curve 2), and $\alpha+\beta$ (curve 3) for $V/\gamma=3$, $\Delta_L=0$, and $\Omega=0$.

we define the strength of the probe signal as $E_\sigma = \mathcal{E}\langle a_\sigma P \rangle$ (\mathcal{E} is the field strength of a single photon). We consider the simplest case: without a magnetic field, i.e., $\Omega=0$. Then $\alpha_\sigma = \alpha_{\sigma'} = \alpha$, and $\beta_\sigma = \beta_{\sigma'} = \beta$. The condition of wave-vector matching is presumed to be satisfied. We assume that the probe wave with left-handed polarization is scattered in beam A2 (see Fig. 1b). Then, using (8), we obtain

$$\frac{d}{dt} E_+ = \alpha E_+ + \beta E_-, \quad (29)$$

$$\frac{d}{dt} E_- = \alpha E_- + \beta E_+. \quad (30)$$

Transforming to partial derivatives

$$\frac{d}{dt} \rightarrow \frac{\partial}{\partial t} + c \frac{\partial}{\partial z}$$

with the boundary conditions $E_+(0) = E_0$, $E_-(0) = 0$, we find the stationary solution for these equations:

$$E_+(z) = \frac{E_0}{2} (e^{\lambda_+ z} + e^{\lambda_- z}), \quad E_-(z) = \frac{E_0}{2} (e^{\lambda_+ z} - e^{\lambda_- z}), \quad (31)$$

where $\lambda_\pm = \bar{\alpha} \pm \bar{\beta}$, $\bar{\alpha} = \alpha/c$, and $\bar{\beta} = \beta/c$. For simplicity, the difference between the phase velocity of wave propagation and the velocity of light c is neglected in the present work. In an optically thin medium, i.e., when $\lambda_\pm z \ll 1$, we obtain $E_+(z) = E_0(1 + \bar{\alpha}z)$, $E_-(z) = E_0\bar{\beta}z$, and for a wave with left-handed polarization $\text{Re } \bar{\alpha}$ may be interpreted as the absorption coefficient. This cannot be done in the general case, since the solution is determined by the scale factor λ_\pm . In intense fields, $\text{Re } \lambda_+$ can change sign (see Fig. 5). We also note that it coincides with the absorption coefficient (gain) of a classical probe signal for two-level atoms in an electromagnetic field with a Rabi frequency $\sqrt{2V}$ (this is also the Rabi frequency for a pump wave interacting with two-level atoms).^{6,17} It follows from solution (31) in the amplification region that in an optically dense medium ($\lambda_\pm z \gg 1$) the amplitudes of the waves equalize, and a growing wave with linear polarization is ultimately obtained.

It follows from this analysis that one significant feature of the system under consideration is the fact that Beer's law does not hold: the absorption coefficient cannot be determined in the usual manner, and the polarization structure of

the radiation varies. The presence of a magnetic field further complicates the situation under consideration.¹¹

4. INFLUENCE OF THE CAVITY ON THE FLUORESCENCE SPECTRA

Let us consider the experimental situation depicted in Fig. 1b, assuming that the scattering system is located in a high- Q Fabry-Perot cavity oriented parallel to the y or z axis. The scattered radiation is selected by the spectral modes of the cavity and then measured by an external detector. We note that a similar experimental setup was used in Ref. 18 to measure resonance fluorescence spectra. We assume that the width of the intracavity modes is sufficiently large in comparison to the total width of the fluorescence spectra not to influence their form.

The scattered radiation is described by Eqs. (10)–(13). We represent them in the following manner:

$$\frac{d}{dt} \mathbf{n} = \mathbf{D}\mathbf{n} + \mathbf{A}, \quad (32)$$

where

$$\mathbf{n} = \begin{pmatrix} n_+ \\ n_- \\ \langle a_+^+ a_+ \rangle \\ \langle a_+^+ a_- \rangle \end{pmatrix}, \quad \mathbf{A} = \begin{pmatrix} \mathcal{A}_{++} \\ \mathcal{A}_{--} \\ \mathcal{A}_{-+} \\ \mathcal{A}_{+-} \end{pmatrix},$$

$$\mathbf{D} = \begin{pmatrix} \alpha'_+ + \alpha'^*_{+} & 0 & \beta^*_+ & \beta_+ \\ 0 & \alpha'_- + \alpha'^*_{-} & \beta_- & \beta^*_- \\ \beta^*_- & \beta_+ & \alpha'_+ + \alpha'^*_{-} & 0 \\ \beta_- & \beta^*_+ & 0 & \alpha'_- + \alpha'^*_{+} \end{pmatrix}.$$

When atoms are irradiated by a laser, the photon number increases until a stationary value is achieved. This state is described by the stationary solution of Eq. (32):

$$\mathbf{n} = \mathbf{D}^{-1} \mathbf{A}. \quad (33)$$

The limit $\omega/Q \gg \kappa_{\sigma\sigma}$, and $\kappa_{\sigma\sigma'}$ corresponds to a low- Q cavity. In this case solution (33) has the form $\mathbf{n} = Q\mathbf{A}/\omega$ and describes expressions (21) and (22) for the spectra in free space. When ω/Q becomes comparable to $\kappa_{\sigma\sigma}$ or $\kappa_{\sigma\sigma'}$, the spectra change significantly. We introduce the parameter $q = \omega/Q\kappa_0$ and investigate the dependence of the scattering spectra on this parameter.

Figure 6 presents plots of the spectral dependence of the photon number n_x , which is stipulated by the inelastic scattering of the pump wave and was calculated from Eqs. (33), (18), and (19) for various values of q . We note that the contribution of the elastic scattering of the laser wave for the parameters corresponding to Fig. 6, as well as Fig. 7, is small. It can be seen from Fig. 6 that the values of n_x , which determine the Hanle signal, may be greatly dependent on the Q factor of the cavity. For the parameters corresponding to the plots in Fig. 6, an increase in the Q factor of the cavity results not only in an increase in the photon number n_x , but also in drastic changes in the spectral composition. With respect to n_y , an increase in the Q factor of the cavity results only in an increase in this photon number, but the spectral

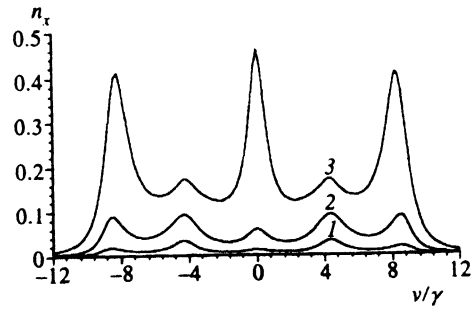


FIG. 6. Spectral dependence of the photon number n_x for $V/\gamma=3$, $\Delta_L=0$, $\Omega/\gamma=1$, and $q=0.5$ (curve 1), 0.1 (curve 2), and 0.02 (curve 3).

composition does not change significantly. A similar dependence, i.e., relative spectral stability as the Q factor of the cavity increases, is exhibited by the numbers of photons with left- and right-handed polarization n_+ and n_- . Significant changes occur in the spectra of these photons only when q becomes considerably closer to its threshold value q_{thr} . The value of q_{thr} is given by the condition

$$\det \mathbf{D} = 0 \quad (34)$$

for at least one frequency ν in the spectral distribution of the photons. Satisfaction of condition (34) or the condition $\det \mathbf{D} < 0$ means that an increase in the Q factor of the cavity and, accordingly, a decrease in q create a situation in which the increase in the photon number begins to surpass the intracavity losses. Then the photon number in the cavity con-

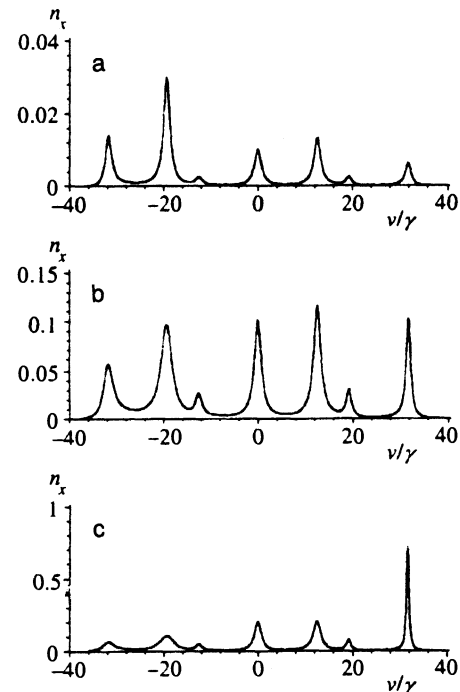


FIG. 7. Spectral dependence of the photon number n_x for $V/\gamma=10$, $\Delta_L/\gamma=-10$, $\Omega/\gamma=5$, and $q=1$ (a), 0.1 (b), and $q=0.05$ (c).

tinually increases, and the stationary regime is violated. Thus, in this case solution (33) does not have any physical meaning.

It was noted in Ref. 1 that the spectrum of the Hanle signal may contain up to seven peaks. The spectra in Fig. 6 contain five features. This is due to the fact that they were calculated under the condition of exact resonance between the pump wave frequency and the transition frequency. In this case the quasienergy spectrum of the atom is equidistant, causing degeneracy of two pairs of peaks in the emission spectrum. A seven-peak structure is clearly displayed when there is considerable detuning from resonance: $\Delta_L > \gamma$. Plots of the spectral dependence were calculated for various values of q under this condition n_x (see Fig. 7). It is noteworthy that the fluorescence spectra considered here, unlike the fluorescence spectra of a two-level atom,⁵ are asymmetric when there is detuning even in an optically thin medium. This is due to the different degrees of excitation of the upper levels.

5. INFLUENCE OF PROPAGATION EFFECTS ON THE FLUORESCENCE SPECTRA

In laser-spectroscopic problems the influence of stimulated processes on the scattering spectra becomes significant when a laser wave acts on extended media. The characteristic features of these processes, which are associated with the propagation of scattered radiation in optically dense media, are investigated in this section with reference to the Hanle effect in the system depicted in Fig. 1b. Here the atomic beams are assumed to be optically dense.

The propagation of scattered radiation is described by the system of equations (10)–(13). The form of this system as presented does not make it possible to obtain analytical solutions convenient for investigation. Therefore, taking into account that the variables in this system are correlators of the creation and annihilation operators, we can represent it in a more symmetric form. For this purpose we introduce the vector \mathbf{G} and the matrix Σ , which have the form

$$\mathbf{G} = \begin{pmatrix} \langle a_+ \rangle \\ \langle a_- \rangle \end{pmatrix}, \quad \Sigma = \begin{pmatrix} n_+ & \langle a_-^+ a_+ \rangle \\ \langle a_+^+ a_- \rangle & n_- \end{pmatrix}. \quad (35)$$

The equations of motion for these quantities can be obtained using Eqs. (8) for the photon field operator P :

$$\frac{d}{dt} \mathbf{G} = \mathbf{K} \mathbf{G}, \quad (36)$$

$$\frac{d}{dt} \Sigma = \mathbf{K} \Sigma + \Sigma \mathbf{K}^\dagger + \mathbf{A}, \quad (37)$$

where the matrices \mathbf{K} and \mathbf{A} have the form

$$\mathbf{K} = \begin{pmatrix} \alpha_+ & \beta_+ \\ \beta_- & \alpha_- - ic\Delta k \end{pmatrix}, \quad \mathbf{A} = \begin{pmatrix} \mathcal{A}_{++} & \mathcal{A}_{+-} \\ \mathcal{A}_{-+} & \mathcal{A}_{--} \end{pmatrix}. \quad (38)$$

Equation (36) describes classical probe fields, and (37) is a modified form of system (10)–(13). Here we have taken into account the special features of the four-wave mixing associated with wave-vector matching condition (9), which has the following form in the geometry under consideration:

$$(k_+ - k_-)l + (k_L - k_{L+})x = 0. \quad (39)$$

Here l describes the y or z coordinate, depending on the direction in which the photons are scattered. This expression reveals that the wave-vector mismatch $\Delta k = k_+ - k_-$ has a significant influence on the propagation of the scattered photons. Making the transition from complete to partial derivatives by performing the replacement

$$\frac{d}{dt} \rightarrow \frac{\partial}{\partial t} + c \frac{\partial}{\partial l},$$

we find the stationary solution of Eq. (37):

$$\Sigma = \exp(\bar{\mathbf{K}}L) \Sigma(0) [\exp(\bar{\mathbf{K}}L)]^\dagger + \int_0^L \exp(\bar{\mathbf{K}}l) \bar{\mathbf{A}} [\exp(\bar{\mathbf{K}}l)]^\dagger dl, \quad (40)$$

where L is the transverse dimension of the atomic beam and $\bar{\mathbf{K}} = \mathbf{K}/c$. The first term in this expression describes the homogeneous solution, for which the vacuum states $\Sigma(0) = \mathbf{I}/2$ can serve as an initial condition. The propagation processes of the scattered radiation per se are described by the second term, which is the subject of our research. We introduce the matrix \mathbf{S} , which diagonalizes $\bar{\mathbf{K}}$:

$$\bar{\mathbf{K}} = \mathbf{S}^{-1} \begin{pmatrix} \lambda_1 & 0 \\ 0 & \lambda_2 \end{pmatrix} \mathbf{S}, \quad (41)$$

where

$$\lambda_{1,2} = [\bar{\alpha}_+ + \bar{\alpha}_- - i\Delta k \pm \sqrt{(\bar{\alpha}_+ - \bar{\alpha}_- + i\Delta k)^2 + 4\beta_+ \beta_-}] / 2.$$

Then for the matrix exponential function we have the expression

$$[\exp(\bar{\mathbf{K}}l)]_{jk} = \sum_{m=1,2} (\mathbf{S}^{-1})_{jm} (\mathbf{S})_{mk} \exp(\lambda_m l), \quad (42)$$

$$[(\exp(\bar{\mathbf{K}}l))^\dagger]_{jk} = (\exp(\bar{\mathbf{K}}l))_{kj}^*. \quad (43)$$

After integrating (40), for the j, k element of the second term Σ in this expression we have

$$(\Sigma^N)_{jk} = \sum_{\substack{m,n, \\ p,q=1,2}} (\bar{\mathbf{A}})_{mn} (\mathbf{S}^{-1})_{jp} (\mathbf{S})_{pm} (\mathbf{S}^{-1})_{kq}^* (\mathbf{S})_{qn}^* \times \frac{\exp[(\lambda_p + \lambda_q^*)L] - 1}{\lambda_p + \lambda_q^*}. \quad (44)$$

We note that the approach used here to solve the system of equations (10)–(33) is similar to the method employed in the work of Agarwal and Boyd¹⁹ to analyze nondegenerate forward four-wave mixing.

Plugging the quantities obtained from solution (44) into Eqs. (18) and (19), we find expressions for n_x and n_y . An analysis of these expressions demonstrates the significant influence of the propagation effects on the scattering spectra. The spectra of the photon number n_x for various values of $\alpha_0 L$ (here α_0 is the unsaturated absorption coefficient of the photons in the line center in the absence of a magnetic field) are presented in Figs. 8a–c. In the case of an optically thin medium (Fig. 8a), the scattering spectrum contains seven

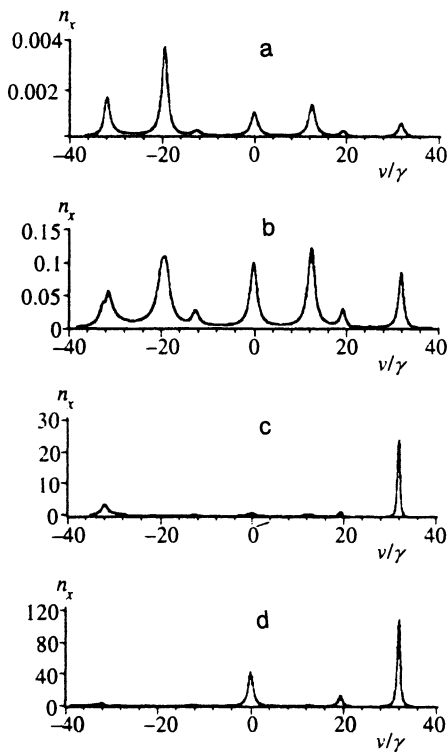


FIG. 8. Spectra of the photon number n_x for $V/\gamma=10$, $\Delta_L/\gamma=-10$, $\Omega/\gamma=5$, and the values $\alpha_0 L=0.1$, $\Delta k=0$ (a), $\alpha_0 L=10$, $\Delta k=0$ (b), $\alpha_0 L=100$, $\Delta k=0$ (c), and $\alpha_0 L=100$, $\Delta k/\alpha_0=0.2$ (d).

components with frequencies $\nu=0, \pm\Omega_j$ ($j=1, 2, 3$). The values of the generalized Rabi frequencies Ω_j are specified by the real parts of the eigenvalues of \mathbf{M} . For the parameters corresponding to Fig. 8, $\Omega_1 \approx 12\gamma$, $\Omega_2 \approx 19\gamma$, and $\Omega_3 \approx 32\gamma$. The high-frequency component corresponding to $\nu \approx \Omega_3$ predominates in the spectra of n_y , n_+ , and n_- when $\alpha_0 L=100$ and $\Delta k=0$ (Fig. 8c). Essentially no displacement of the positions of the component maxima in the scattering spectra occurs as the optical thickness increases. This is attributed to the fact that the features in the radiation gain factors, like the

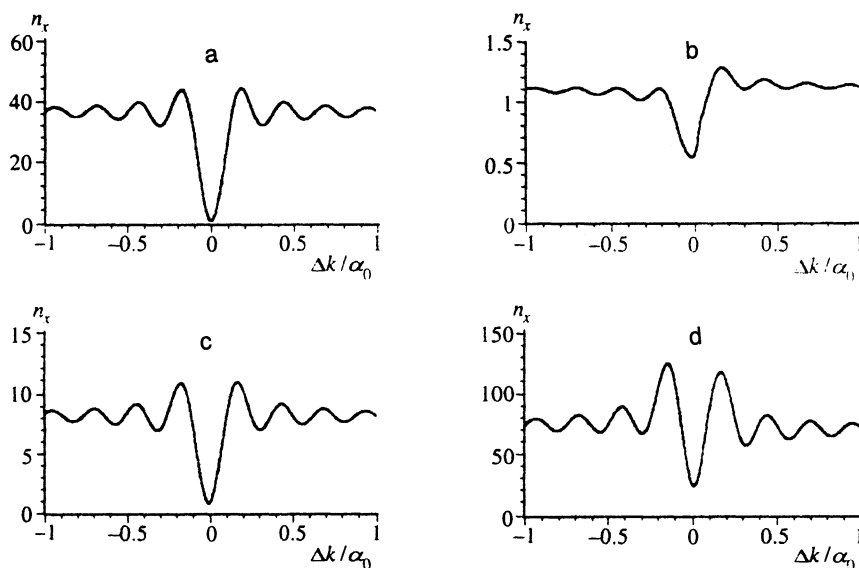


FIG. 10. Dependence of the photon number n_x on the magnitude of the wave-vector mismatch Δk for $\nu=0$ (a) $\nu=\Omega_1$ (b), $\nu=\Omega_2$ (c), and $\nu=\Omega_3$ (d) when $V/\gamma=10$, $\Delta_L/\gamma=-10$, $\Omega/\gamma=5$, and $\alpha_0 L=100$.

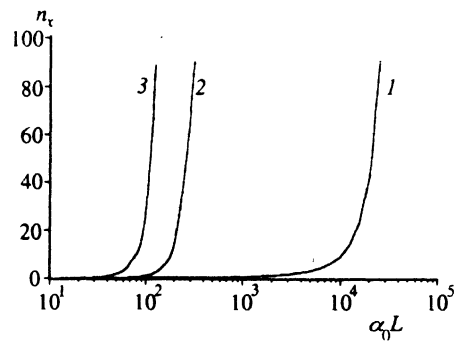


FIG. 9. Dependence of the photon number n_x on the optical thickness $\alpha_0 L$ for $\nu=\Omega_1$ (curve 1), $\nu=\Omega_2$ (curve 2), and $\nu=\Omega_3$ (curve 3) when $V/\gamma=10$, $\Delta_L/\gamma=-10$, $\Omega/\gamma=5$, and $\Delta k=0$.

peaks in the spontaneous scattering spectra of the atoms, are located near generalized Rabi frequencies. When the incident wave is detuned from resonance, the amplification of the scattered radiation exhibits asymmetry. This is the reason why the high-frequency components dominate in the scattering spectrum at large optical thicknesses when there is low-frequency detuning of the pump wave from resonance (Fig. 8c). The preferential growth of these components can also be seen in Fig. 9, which presents the dependence of n_x on $\alpha_0 L$ for $\nu=\Omega_j$ ($j=1, 2, 3$).

Figures 8a–c were plotted for the condition of exact wave-vector matching $\Delta k=0$. The presence of some mismatch $\Delta k \neq 0$ significantly alters the gain factors. Plots of the dependence of the photon number n_x for $\nu=0, \Omega_j$ ($j=1, 2, 3$) on the magnitude of the wave-vector mismatch are presented in Fig. 10. The dependence of n_x on Δk for the low-frequency components with $\nu=-\Omega_j$ is less abrupt than the dependence in Fig. 10. The influence of the wave-vector mismatch on the spectrum of n_x is demonstrated in Figs. 8c and d, the latter of which was plotted for $\Delta k=0.2\alpha_0$ and the same values for the other parameters.

The foregoing analysis focused on an investigation of

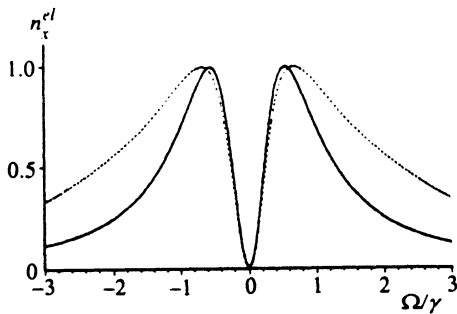


FIG. 11. Dependence of the photon number n_x^{el} on Ω (the magnetic field strength) for $V/\gamma=0.1$, $\Delta_L/\gamma=-10$, $\Delta k=0$, and $\alpha_0 L=0.1$ (solid line) and 20 (dashed line). The plots have been normalized at their maxima to unity.

the influence of propagation effects on the inelastic component of the fluorescence spectra, which, as was noted above, is dominant in strong fields. Let us now consider the influence of these effects on the coherent component $n_x^{el} \propto \mathcal{R}(\nu)$. In an optically thin medium $n_x^{el} \propto \mathcal{A}_x^{el}$. The dependence of n_x^{el} on the optical thickness $\alpha_0 L$ is specified by relation (18) and solution (44), for which the components $\mathcal{A}_{\sigma\sigma'}$ of \mathbf{A} retain only the expressions describing elastic scattering $\mathcal{A}_{\sigma\sigma'}^{el}$ [see (27)]. The influence of $\alpha_0 L$ on the dependence of n_x^{el} on the magnetic field strength is shown in Fig. 11 for the weak-field case ($V/\gamma=0.1$) and in Fig. 12 for the strong-field case ($V/\gamma=10$) with the parameters $\Delta_L/\gamma=-10$ and $\Delta k=0$. It can be seen from Fig. 11 that the stimulated processes have a significant influence when the intensity of the pump wave is low only if the magnetic field is fairly strong ($\Omega > \Delta_L, \gamma$). This fact is of special importance, since the elastic component of the scattering is dominant and essentially completely determines the overall Hanle signal when $V \ll \gamma$. This means that the width of the dip in the Hanle profile scarcely depends on the optical thickness. This conclusion is significant in experimental investigations, where the magnitude of this dip is used to determine the properties of the atomic subsystem and the features of its interaction with the radiation. Conversely, in strong fields $V \gg \gamma$ (see Fig. 12), the influence of the stimulated processes on the coherent component is displayed most conspicuously at relatively weak magnetic fields $\Omega \leq V$. Observing this factor is hampered by the fact

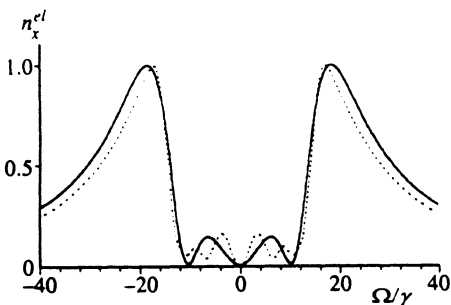


FIG. 12. Dependence of the photon number n_x^{el} on Ω (the magnetic field strength) for $V/\gamma=10$, $\Delta_L/\gamma=-10$, $\Delta k=0$, and $\alpha_0 L=0.1$ (solid line) and 400 (dashed line). The plots have been normalized at their maxima to unity.

that the elastic component is considerably weaker than the inelastic component. We note that the dependences in Figs. 11 and 12 were calculated for the condition of exact wave-vector matching. The formal calculation of these plots at a fixed value of $\Delta k \neq 0$ is incorrect. This is due to the fact that the propagation of photons in this system obeys the dispersion relation

$$(\epsilon_+ \omega^2 - c^2 k_+^2)(\epsilon_- \omega^2 - c^2 k_-^2) - \omega^2 \beta_+ \beta_- = 0, \quad (45)$$

where $\epsilon_\sigma = 1 + \alpha_\sigma/\omega$ is the dielectric constant for a σ -polarized wave without consideration of the four-wave mixing. In zero magnetic field the coefficients with indices + and - are identical, and the equality $\Delta k=0$ becomes necessary. The formal introduction of some wave-vector mismatch $\Delta k \neq 0$ in this case results in different phase velocities of wave propagation and, ultimately, in the disappearance of the level-crossing effect. An analysis shows that in strong magnetic fields, Δk can vary over a broad range ($\Delta k=0$ to $0.5 \alpha_0$) without having an appreciable influence on the elastic component of the Hanle signal. We note that in the general case, even for the inelastic component of the Hanle signal, the possibility of varying Δk is restricted by the condition that equality (45) must be satisfied.

For the case of observation of the Hanle effect in gaseous media, which is often utilized experimentally, we add that the proposed approach should be expanded by taking into account such factors as the nonuniform distribution of the field in any cross section of the laser beam, the thermal motion, and the absorption of radiation upon passage through a region of atomic vapor not perturbed by laser radiation.

6. CONCLUSIONS

It has been shown in the present study that the spectral and polarization properties of the fluorescence of atoms excited by a monochromatic wave in a magnetic field may be influenced significantly by stimulated processes. Their role becomes appreciable if the atomic system is optically dense. The spectra of the absorption and four-wave mixing coefficients, which determine the dynamics of the stimulated processes, have been investigated in this work. The special features of the probe-wave method as applied to the system considered have been established.

We have singled out the role of four-wave mixing processes in the foregoing analysis of the influence of stimulated processes on fluorescence spectra, particularly on spectra of the Hanle signal, which was investigated in detail in this study. While the influence of stimulated absorption and emission processes is generally obvious, the presence of four-wave mixing is not a trivial matter. The investigation of the Hanle effect in Ref. 1 showed that it is of fundamental significance for describing interference phenomena in optically thin systems. The role of four-wave mixing processes becomes even more important in optically dense systems. This is due not only to the dynamics of the propagation of the scattered waves, but also to the special features of the phase matching in four-wave mixing.

In the description we developed it was not assumed that the pump wave is small, and in the resonance approximation our theory maintains its generality for a monochromatic wave of arbitrary intensity.

One of us (A.A.P.) thanks the Russian Fund for Fundamental Research for partial financial support of this work (Grant No. 94-02-05853-a).

¹F. A. Lomaya and A. A. Panteleev, *Zh. Eksp. Teor. Fiz.* **103**, 1970 (1993) [*JETP* **76**, 976 (1993)].

²W. Hanle, *Z. Phys.* **30**, 93 (1924).

³E. B. Aleksandrov, G. I. Khvostenko, and M. P. Chaika, *Interference of Degenerate Atomic States* [in Russian], Nauka, Moscow (1991).

⁴S. G. Rautian and I. I. Sobel'man, *Zh. Eksp. Teor. Fiz.* **41**, 456 (1961) [*Sov. Phys. JETP* **14**, 328 (1962)].

⁵B. R. Mollow, *Phys. Rev.* **188**, 1969 (1969).

⁶B. R. Mollow, *Phys. Rev. A* **5**, 2217 (1972).

⁷P. Avan and C. Cohen-Tannoudji, *J. Phys. Lett.*, **36**, L85 (1975).

⁸S. P. Goreslavskii and V. P. Kraĭnov, *Zh. Eksp. Teor. Fiz.* **80**, 467 (1981) [*Sov. Phys. JETP* **53**, 328 (1981)].

⁹G. Vemuri, M. H. Anderson, J. Cooper *et al.*, *Phys. Rev. A* **44**, 7635 (1991).

¹⁰D. A. Holm, M. Sargent III, and S. Stenholm, *J. Opt. Soc. Am. B* **2**, 1456 (1985).

¹¹A. A. Panteleev, *Zh. Eksp. Teor. Fiz.* **99**, 1684 (1991) [*Sov. Phys. JETP* **72**, 939 (1991)].

¹²M. Sargent III, D. A. Holm, and M. S. Zubairy, *Phys. Rev. A* **31**, 3112 (1985).

¹³S. Stenholm, D. A. Holm, and M. Sargent III, *Phys. Rev. A* **31**, 3124 (1985).

¹⁴M. O. Scully and W. E. Lamb, Jr., *Phys. Rev.* **159**, 208 (1967).

¹⁵W. Rasmussen, R. Schieder, and H. Walther, *Opt. Commun.* **12**, 315 (1974).

¹⁶L. D. Landau and E. M. Lifshitz, *Electrodynamics of Continuous Media*, Pergamon, Oxford (1983).

¹⁷S. G. Rautian, G. I. Smirnov, and A. M. Shalagin, *Nonlinear Resonance in Atomic and Molecular Spectra* [in Russian], Nauka, Novosibirsk (1979).

¹⁸W. Hartig, W. Rasmussen, R. Schieder *et al.*, *Z. Phys. A* **278**, 205 (1976).

¹⁹G. S. Agarwal and R. W. Boyd, *Phys. Rev. A* **38**, 4019 (1988).

Translated by P. Shelnitz